Article

FORMATION OF SAWTOOTH WAVES FOR CYLINDRICAL AND SPHERICAL KORTWEG-DE VRIES-BURGERS EQUATIONS

Alexey Samokhin [1] 0000-0003-1352-2839

[1] Trapeznikov Institute of Control Scienties, Russian Academy of Sciences, 65 Profsoyuznaya street, 117997 Moscow, Russia; samohinalexey@gmail.com

Abstract: For the KdV-Burgers equations on cylindrical and spherical waves the development of a regular profile starting from an equilibrium under a periodic perturbation at the boundary is studied. The equations describe a medium which is both dissipative and dispersive. Symmetries, invariant solutions and conservation laws are investigated. For an appropriate combination of dispersion and dissipation the asymptotic profile looks like a periodical chain of shock fronts with a decreasing amplitude (sawtooth waves). The development of such a profile is preceded by a head shock of a constant height and equal velocity which depends on spatial dimension as well as on integral characteristics of boundary condition; an explicit asymptotic for this head shock and a median of the oscillating part is found.

Keywords: Korteweg-de Vries-Burgers equation; cylindrical and spherical waves; saw-tooth solutions; periodic boundary conditions; head shock wave.

MSC: 35Q53, 35B36

---

1. Introduction

The behavior of solutions of the KdV and KdV - Burgers equations is well studied, yet they remain a subject of various recent research, [3]–[6] where these equations describe flat waves in one spatial dimension. But less studied cylindrical and spherical waves have a variety applications (eg, waves generated by a downhole vibrator).

The well known KdV-Burgers equation for flat waves is of the form

$$u_t = -2uu_x + \varepsilon^2 u_{xx} + \delta u_{xxx}. \tag{1}$$

Its cylindrical and spherical analogues are

$$u_t + \frac{1}{2t}u = -2uu_x + \varepsilon^2 u_{xx} + \delta u_{xxx}. \tag{2}$$

and

$$u_t + \frac{1}{t}u = -2uu_x + \varepsilon^2 u_{xx} + \delta u_{xxx}. \tag{3}$$

correspondingly, see [1] – [2].

We consider the initial value - boundary problem (IVBP) for the KdV-Burgers equation on a finite interval:

$$u(x,0) = f(x),\ u(a,t) = l(t),\ u(b,t) = L(t),\ u_x(b,t) = R(t),\ x \in [a,b]. \tag{4}$$

In the case $\delta = 0$ (that is, for Burgers equation), it comes to

$$u(x,0) = f(x),\ u(a,t) = l(t),\ u(b,t) = R(t),\ x \in [a,b]. \tag{5}$$

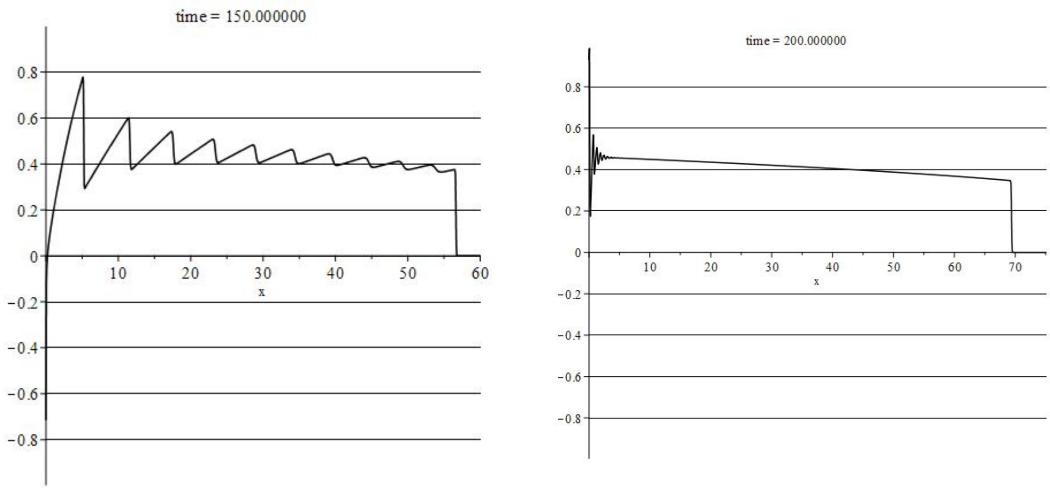

Figure 1. *Cylindrical Burgers,* $\varepsilon = 0.1$, ***Left****:* $u_0 = \sin t, t = 150$. ***Right****:* $u_0 = \sin 10t, t = 200$.

The case of the boundary conditions $u(a,t) = A\sin(\omega t),\ u(b,t) = 0$ and the related asymptotics are of a special interest here. For numerical modelling we use $x \in [0,b]$ instead of $\mathbb{R}^+$ for appropriately large b.

This paper is a continuation of the previous research by the author, [7] – [12].

2. Flat case: travelling waves

For $t \gg 1$ equations (2) and (3) tend to (1) as well as do their solutions. In particular, the explicit form of traveling wave solutions for the flat KdV-Burgers (1) is as follows

$$u_{\text{tws}}(x,t) = \frac{3\varepsilon^4 \tanh^2\left(\frac{\varepsilon^2(x-Vt-s)}{10\delta}\right)}{50\delta} - \frac{3\varepsilon^4 \tanh\left(\frac{\varepsilon^2(x-Vt-s)}{10\delta}\right)}{25\delta} + \frac{V}{2} - \frac{3\varepsilon^4}{50\delta} \tag{6}$$

Our IVBP requires $u|_{x=+\infty} = 0$; so the sole such travelling wave has a velocity $V = \frac{6\varepsilon^4}{25\delta}$.

Note that the height of the wave (6), $u|_{x=-\infty} - u|_{x=+\infty} = H - h = 6\varepsilon^4/25\delta$ does not depend on its velocity and is completely defined by the ratio ε^4/δ which depends on the coefficients $\varepsilon,\ \delta$ related to dispersion and dissipation.

Also note that the equations (1)–(3) may be readily put in the form $w_t + \frac{n}{2t}w = \gamma w_{xx} - 2ww_x + w_{xxx}$ by the change of variables $t \to t\sqrt{\delta},\ x \to x\sqrt{\delta},\ u \to -\frac{u}{2}$. Here $\gamma = \frac{\varepsilon^2}{\sqrt{\delta}}$ is the important parameter that defines a character of solutions; $n = 0, 1/2, 1$ for flat, cylindrical and spherical waves correspondingly.

In the case $\delta = 0$, the Burgers equation has a variety of travelling wave solutions, vanishing at $x \to +\infty$. They are given by the formula

$$u_{\text{Btws}}(x,t) = \frac{V}{2}\left[1 - \tanh\left(\frac{V}{2\varepsilon^2}(x - Vt + s)\right)\right] \tag{7}$$

We demonstrate that in the case of the above IVBP, the perturbation of the equilibrium state for (2), (3) ultimately becomes similar to the form of this shock.

3. Typical examples

3.1. Burgers.

Here we demonstrate typical graphs for cylindrical and spherical Burgers waves, see Figure 1, 2.

Preprints (www.preprints.org) | NOT PEER-REVIEWED | Posted: 23 December 2020 doi:10.20944/preprints202012.0579.v1

3.2. KdV-Burgers.

Typical graphs for cylindrical and spherical KdV-Burgers, Figure 3, 4.

3.3. Overview of examples.

- Stronger viscosity effectively damps oscillation and may result in absence of sawtooth effects.
- Greater frequencies of initial perturbation results in much faster decay.
- A vibration of a greater amplitude results in increase of velocity and amplitude of travelling signal.
- Cylindrical wave moves faster and decay slower than the spherical wave with the same periodical border condition.
- Greater dispersion coefficient δ leads to a more prominent oscillations at the bottom of each tooth (at the place of the derivative breaks).
- After the decay of initial oscillations, graphs become monotonic declining convex lines, terminating by a shock.

4. Symmetries and conservation laws

4.1. Symmetries

Since cylindrical and spherical equations explicitly depend on time, their stock of symmetries is scarce.

The algebras of classical symmetries are generated by the following vector fields:

$$\begin{aligned} X &= \frac{\partial}{\partial x}, \\ Y &= x\frac{\partial}{\partial x} + 2t\frac{\partial}{\partial t} - u\frac{\partial}{\partial u}, \\ Z &= \sqrt{t}\frac{\partial}{\partial x} + \frac{1}{4\sqrt{t}}\frac{\partial}{\partial u}, \\ W &= \ln(t)\frac{\partial}{\partial x} + \frac{1}{2t}\frac{\partial}{\partial u}. \end{aligned}$$

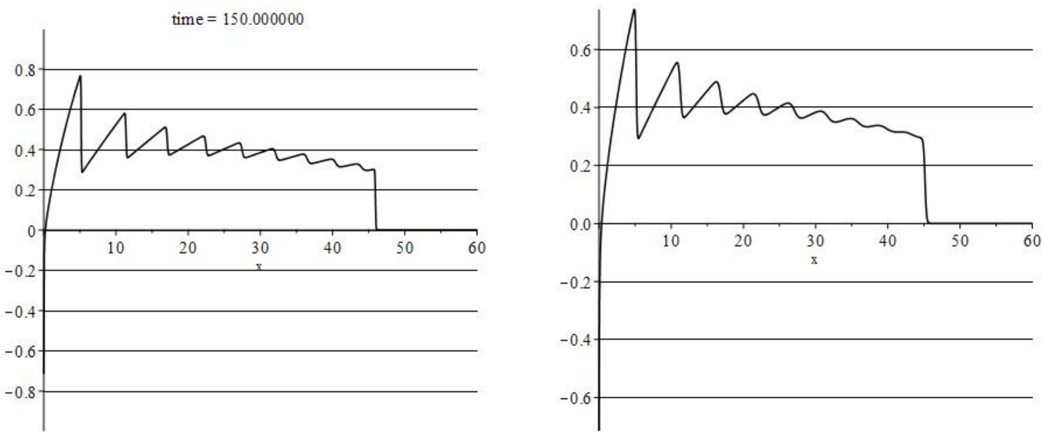

Figure 2. *Spherical Burgers,* $u_0 = \sin t$*, **Left**:* $\varepsilon = 0.1, t = 150$ ***Right***: $\varepsilon^2 = 0.3, t = 150$

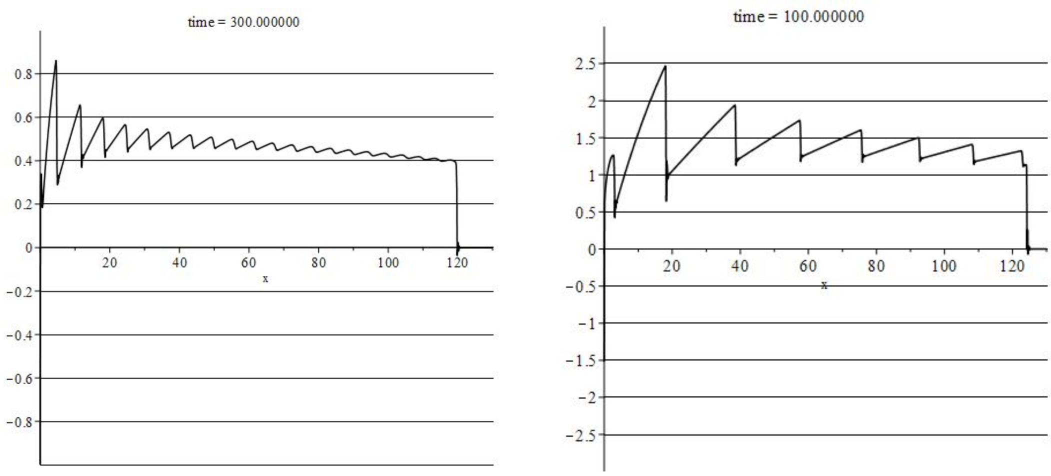

Figure 3. *Cylindrical KdV-Burgars, **Left**:* $u_0 = \sin t, t = 300, \varepsilon = 0.1, \delta = 0.001$.***Right**:* $u_0 = 3\sin t, t = 100, \varepsilon = 0.1, \delta = 0.001$.

It is not hard to find invariant solutions for X, Z and W symmetries. For the Y symmetry an invariant solution must have a form $x^{-1}f(\frac{t}{x^2})$ where $f(\xi)$ is, for a spherical Burgers, a solution of the nonlinear ordinary differential equation

$$f'' + \frac{1}{\varepsilon^2\xi}ff' + \left(\frac{2.5}{\xi} - \frac{1}{4\xi^2\varepsilon^2}\right)f' + \frac{1}{2\xi^2\varepsilon^2}f^2 + \left(\frac{1}{2\xi^2} - \frac{1}{4\xi^3\varepsilon^2}\right)f = 0.$$

Its general solution is not known. With the scaling symmetry for the cylindrical Burgers equation the situation is analogous. Results on invariant solutions are collected in Table 1.

Table 1. Invariant solutions.

Equation	Symmetries	Invariant solutions
Cylindrical Burgers	X, Y, Z	$\frac{C}{\sqrt{(t)}}, \frac{(x+4C)}{4t}, x^{-1}f(\frac{t}{x^2})$ for some f
Cylindrical KdV-Burgers	X, Z	$\frac{C}{\sqrt{(t)}}, \frac{(x+4C)}{4t}$
Spherical Burgers	X, Y, W	$\frac{C}{t}, \frac{x+2C}{2t\ln(t)}, x^{-1}f(\frac{t}{x^2})$ for some f
Spherical KdV-Burgers	X, W	$\frac{C}{t}, \frac{x+2C}{2t\ln(t)}$

4.2. Conservation laws

First rewrite equations (1) – (3) into an appropriate, conservation law form

$$[t^n \cdot u]_t = [t^n \cdot (-u^2 + \varepsilon^2 u_x + \delta u_{xx})]_x, \tag{8}$$

where $n = 0,\ 1/2,\ 1$ for flat, cylindrical and spherical cases correspondingly.

Hence for solutions of the above equations we have

$$\oint\limits_{\partial\mathcal{D}} t^n \cdot [u\,dx + (\varepsilon^2 u_x - u^2 + \delta u_{xx})\,dt] = 0, \tag{9}$$

where $\mathcal{D}$ is a rectangle

$$\{0 \leq x \leq L,\ 0 \leq t \leq T\}.$$

Bearing in mind the initial value/boundary conditions $u(x,0) = u(+\infty,t) = 0$, for $L = +\infty$ the integrals read

$$\int_{+\infty}^{0} T^n u(x,T)\,dx + \int_{T}^{0} t^n(\varepsilon^2 u_x(0,t) - u^2(0,t) + \delta u_{xx}(0,t))\,dt = 0.$$

Thus

$$\int_{0}^{+\infty} u(x,T)\,dx = \frac{1}{T^n}\int_{0}^{T} t^n(-\varepsilon^2 u_x(0,t) + u^2(0,t) - \delta u_{xx}(0,t))\,dt. \tag{10}$$

Subsequently

$$\frac{1}{T}\int_{0}^{+\infty} u(x,T)\,dx = \frac{1}{T}\int_{0}^{T} \frac{1}{T^n} t^n(-\varepsilon^2 u_x(0,t) + u^2(0,t) - \delta u_{xx}(0,t))\,dt. \tag{11}$$

The right-hand side of (11) is the mean value right-hand side of (10).

It can be computed in some simple cases or estimated. for instance, assume that $\varepsilon^2 u_x(0,t) + \delta u_{xx}(0,t)$ is negligible compared to $u^2(o,t)$. Then

$$\frac{1}{T}\int_{0}^{+\infty} u(x,T)\,dx \approx \frac{1}{T}\int_{0}^{T} \frac{1}{T^n} t^n(u^2(0,t))\,dt = \frac{1}{T}\int_{0}^{T} \frac{1}{T^n} t^n(A\sin^2(\omega t))\,dt. \tag{12}$$

It follows that

$$n = 0 \Rightarrow \lim_{T\to\infty} \tfrac{1}{T}\int_0^T A^2\sin^2(\omega t)\,dt = \lim_{T\to\infty} \tfrac{A^2}{2\omega T}(\omega T - 0.5\sin(2\omega T)) = \tfrac{A^2}{2};$$

$$n = \tfrac{1}{2} \Rightarrow \lim_{T\to\infty} \tfrac{1}{T}\int_0^T \tfrac{1}{T^{\frac{1}{2}}} t^{\frac{1}{2}}(A\sin^2(\omega t)\,dt =$$

$$\lim_{T\to\infty} \tfrac{A^2}{24\sqrt{\omega^3 T^3}}\left(8(\omega T)^{\frac{3}{2}} - 6\sqrt{\omega T}\sin(2\omega T) + 3\sqrt{\pi}\,\mathrm{FresnelS}(\tfrac{2\sqrt{\omega T}}{\sqrt{\pi}}\right) = \tfrac{A^2}{3};$$

$$n = 1 \Rightarrow \lim_{T\to\infty} \tfrac{1}{T}\int_0^T \tfrac{1}{T} t(A^2\sin^2(\omega t)\,dt = \lim_{T\to\infty} \tfrac{A^2}{4\omega^2 T^2}\left(-\omega T\sin(2\omega T) + \omega^2 T^2 + \sin^2(\omega T)\right) = \tfrac{A^2}{4}.$$

4.3. Constant boundary conditions

Consider boundary condition $u(0,t) = M$. The graphs of solution are shown on Figure 5, left (compare their rate of decay caused solely by the spaces dimensions.)

For the resulting compression wave $u_x(0,t) = 0$ and the right-hand side of (11) equals

$$\frac{1}{T}\int_{0}^{T} \frac{M^2}{T^n} t^n\,dt = \frac{M^2}{n+1} \tag{13}$$

As the Figures 1 — 4 show, for periodic boundary condition, after the decay of initial oscillations, graphs become monotonic convex lines that begin approximately at the hight $A/2$ and broking at $x = V \cdot T$ and at the height V. These monotonic lines are similar to the graphs of constant-boundary solutions, see Figure 5.

Preprints (www.preprints.org) | NOT PEER-REVIEWED | Posted: 23 December 2020 doi:10.20944/preprints202012.0579.v1

4.4. "Homothetic" approximations to solutions

Looking at the solution's graphs one can clearly see (eg, on Figure 5, right) that the monotonic part and its head shock develops as a homothetic transformation of the initial configuration. So we seek solutions of the form $u(x,t) = y(\frac{x}{t})$. Substituting it into equations (1) – (3) we get the equation

$$-y'\frac{x}{t^2} + \frac{ny}{t} = \frac{2yy'}{t} + \frac{\varepsilon^2 y''}{t^2} + \frac{\delta y'''}{t^3}, \tag{14}$$

or

$$-\xi y' + ny = 2yy' + \frac{\varepsilon^2 y''}{t} + \frac{\delta y'''}{t^2}, \tag{15}$$

for $y = y(\xi)$ and $n = 0,\ 1/2,\ 1$. For t large enough we may omit last two summands. It follows that appropriate solutions of these truncated ordinary differential equations are

$$u_1(x,t) = C_1,\ C_1 \in \mathbb{R},\ n = 0,\ \text{for flat waves equation;}$$

$$u_2(x,t) = -\frac{2 + \sqrt{C_2\xi + 4}}{C_2},\ C_2 \in \mathbb{R},\ n = \frac{1}{2},\ \text{ for cylindrical and}$$

$$u_3(x,t) = \exp\left(\text{LambertW}\left(-\frac{\xi}{2}e^{-\frac{C_3}{2}}\right) + \frac{C_3}{2}\right),\ C_3 \in \mathbb{R},\ n = 1 \text{ for spherical equation.}$$

Let V be the velocity of the signal propagation in the medium. Since at the head shock $x = Vt$ and $u = V$ we obtain the condition for finding C_i. It is $y(V) = V$. It follows then that

$$C_1 = V,\ C_2 = -\frac{3}{V},\ C_3 = \ln(V) + \frac{1}{2}.$$

For flat waves it corresponds to a travelling wave solution of the classical Burgers equation. For the cylindrical waves the monotonic part is given by

$$u_2 = \frac{1}{3}\left(2V + V\sqrt{4 - \frac{3x}{Vt}}\right);$$

for spherical waves

$$u_3 = V\sqrt{e}\exp\left(\text{LambertW}\left(-\frac{x}{2Vt\sqrt{e}}\right)\right).$$

Note that

$$u_2|_{x=0} = \frac{4V}{3} \text{ and } u_3|_{x=0} = V\sqrt{e} \approx 1.65V. \tag{16}$$

These formulas show that the velocity is proportional to the amplitude at the start of oscillation. And it does not depend on frequency that together with amplitude define the oscillating part of solutions; more on that below.

The corresponding graphs visually coincide with the graphs obtained by numerical modelling; for instance see comparison to the solution (at $t = 100$) for the problem

$$u_t = 0.01u_{xx} - 2uu_x - u/t,\ u(0,t) = 1, u(75,t) = 0, u(x,0) = 0 \tag{17}$$

on Figure 6, left.

Yet the smooth part of the periodic boundary solution ends with a break, which travels with a constant velocity and amplitude, very much like a head of the Burgers' travelling wave (TWS) solution

 doi:10.20944/preprints202012.0579.v1

(7). A rather natural idea is to truncate a homothetic solution, multiplying it by a (normalized) Burgers TWS. Namely, put

- For the cylindrical waves take

$$\tilde{u}_2 = \frac{1}{2}[1 - \tanh(\frac{V}{\varepsilon^2}(x - Vt))] \cdot \frac{1}{3}\left(2V + V\sqrt{4 - \frac{3x}{Vt}}\right); \tag{18}$$

- for spherical waves —

$$\tilde{u}_3 = \frac{1}{2}[1 - \tanh(\frac{V}{\varepsilon^2}(x - Vt))] \cdot V\sqrt{e}\exp\left(\mathrm{LambertW}\left(-\frac{x}{2Vt\sqrt{e}}\right)\right). \tag{19}$$

This construction produces an approximation of an astonishing accuracy, see Figure 6, right and Figure 7; these graphs correspond to the spherical KdV-Burgers problem (it comes from (3) after the change $x \to -x$.

$$u_t = 0.02u_{xx} + 2uu_x - u/2t - 0.002u_{xxx}, \; u(0,t) = \sin t, u(10,t) = 0, u(x,0) = 0. \tag{20}$$

Moreover, it is evident that the graphs of $\tilde{u}_2$, $\tilde{u}_3$ neatly represent the median lines of the approximated solutions on their whole range. By median we mean

$$M(x) = (2\pi n/\omega)^{-1}\int_0^{2\pi n/\omega} u(x,t)\,dt, \quad n \in \mathbb{N},\ n \gg 1\ (u(0,t) = \sin\omega t).$$

Now evaluate the trapezoid area under $\tilde{u}_2$, $\tilde{u}_3$ graphs:

- For cylindrical equation

$$\int_0^{Vt}\left[\frac{[1 - \tanh(\frac{V}{\varepsilon^2}(x - Vt))]}{2}\frac{1}{3}\left(2V + V\sqrt{4 - \frac{3x}{Vt}}\right)\right]dx = \frac{32}{27}V^2 t;$$

- for spherical equation

$$\int_0^{Vt}\left[\frac{[1 - \tanh(\frac{V}{\varepsilon^2}(x - Vt))]}{2}V\sqrt{e}\exp\left(\mathrm{LambertW}\left(\frac{-x}{2Vt\sqrt{e}}\right)\right)\right]dx = \frac{V^2 t \cdot e}{2}.$$

Hence the mean value of the left-hand side of (11) can be estimated as follows. Since the signal from $x = 0$ spreads, after decay of oscillations, to the right with a constant speed V and the same constant amplitude V at the shock, and it is very well approximated by an appropriate homothetic solution, we get

$$\frac{1}{T}\int_0^{+\infty} u(x,T)\,dx = \frac{1}{T}\int_0^{VT} u(x,T)\,dx \approx \begin{cases} \frac{32}{27}V^2 \text{ in cylindrical case;} \\ \frac{V^2 \cdot e}{2} \text{ in spherical case,} \end{cases} \tag{21}$$

This mean value can be also evaluated numerically. In the case illustrated by Figure 1 the direct numerical evaluation differs from the estimation (21) by 1%.

For constant-boundary waves, it follows from (13) that

$$\frac{M^2}{n+1} = \begin{cases} \frac{32}{27}V^2 \text{ in cylindrical case;} \\ \frac{V^2 \cdot e}{2} \text{ in spherical case,} \end{cases} \tag{22}$$

see (13); of course this result coincides with (16). So the mean value M of arbitrary solution at the start of oscillations (or in a vicinity of the oscillator) is linearly linked to the velocity of the head shock.

But to find this mean value for an arbitrary border condition is a tricky task, because the integrands u_x and u_{xx} of the right-hand side of (11) have numerous breaks. Still one may get an (admittedly rough) estimation for M using (12) and (22). It follows that

$$\frac{M^2}{n+1} \approx \frac{A^2}{k}, \quad k = 2,\ 3,\ 4 \tag{23}$$

for flat, cylindrical and spherical cases. In all these cases it results in $M \approx A\frac{\sqrt{2}}{2} \approx 0.71A$.

Numerical experiments also show (eg, see Figure 3), that for the $u|_{x=0} = A\sin(t)$ boundary condition such a value is $M \approx A \cdot a$, where $a \approx 0.467$ is the mean value for $1 \cdot \sin(t)$ condition. That is, M depends on A almost linearly.

Note, that this value may be obtained via the velocity of the head shock, which, in its turn, can be measured with great accuracy by the distance passed by the head shock after a sufficiently long time.

5. Discussion

Symmetries, invariant solutions and conservation laws were investigated. We obtained a way to foretell the form of the head shock with a great accuracy: the links in the chain of causations are as follows. First, using the boundary conditions we find, if approximately, the initial mean value of the solution by the formula (23). This value defines the form of the declining homothetic part of the solution, in particular its velocity and median line. When the amplitude of this declining part reaches the value if velocity, the solution jumps to zero value by the scenario of the Burgers travelling wave and becomes a part of a homothetic head shock. In vicinity of the boundary oscillations occur around this homothetic line; their longevity, both in time and space, and whether they have a sawtooth form, is defined by the relations between the amplitude and frequency of forcing oscillations as well as by viscosity and dispersive characteristics of the media. The exact dependencies are now investigated; results will be published elsewhere.

6. Methods

The figures in this paper were generated numerically using Maple PDETools package. The mode of operation uses the default Euler method, which is a centered implicit scheme, and can be used to find solutions to PDEs that are first order in time, and arbitrary order in space, with no mixed partial derivatives.

Funding: This work was partially supported by the Russian Basic Research Foundation grant 18-29-10013.

Conflicts of Interest: The author declares no conflict of interest.

Abbreviations

The following abbreviations are used in this manuscript:

KdV	Kortweg - de Vries
IVBP	Initial value | boundary problem
TWS	Travelling wave solution

References

1. Leibovich S, Seebass R. (Editors). Nonlinear waves, Ch.4 Cornell University Press, Ithaka and London, 1974.
2. Sachdev P.L., Seebas R. Propagation of spherical and cylindrical N-waves. *Journ of Fluid . Mech.* **1973** *58*, 1973.
3. Grava T. Whitham modulation equations and application to small dispersion asymptotics and long time asymptotics of nonlinear dispersive equations. **31 Dec 2016** *arXiv:1701.00069v1 [math-ph]*

 doi:10.20944/preprints202012.0579.v1

4. Chugainova A. P., Shargatov V. A. Traveling waves and undercompressive shocks in solutions of the generalized Korteweg–de Vries–Burgers equation with a time-dependent dissipation coefficient distribution. *Eur. Phys. J. Plus* **2020** *135:635* https://doi.org/10.1140/epjp/s13360-020-00659-3
5. Bendaasa S. Alaa N. Periodic Wave Shock Solutions of Burgers Equations, A New Approach. *Int. J. Nonlinear Anal. Appl.* **2020** *10: 1*, 119–129 http://dx.doi.org/
6. Chugainova1 A. P., Shargatov V. A. Stability of the breaks structure described by the generalized Kortweg-de Vries-Burgers equation. *Computational Math and Math Phys.* **2016** *56:2*, 259–274
7. Samokhin A.V. Soliton transmutations in KdV—Burgers layered media. *Journal of Geometry and Physics* **2020**, *148*, 9 p. https://doi.org/10.1016/j.geomphys.2019.103547
8. Samokhin A.V. Reflection and refraction of solitons by the KdV–Burgers equation in nonhomogeneous dissipative media. *Theoretical and Mathematical Physics* **2018** *197(1)*, 1527–1533. DOI: 10.1134/S0040577918100094
9. Samokhin A. Nonlinear waves in layered media: solutions of the KdV — Burgers equation. *Journal of Geometry and Physics* **2018,** *130*, 33–39. https://doi.org/10.1016/j.geomphys.2018.03.016
10. Samokhin A. On nonlinear superposition of the KdV-Burgers shock waves and the behavior of solitons in a layered medium. *Journal of Differential Geometry and its Applications* **2017** *54, Part A*, 91–99. https://doi.org/10.1016/j.difgeo.2017.03.001
11. Samokhin A. Periodic boundary conditions for KdV-Burgers equation on an interval. *Journal of Geometry and Physics* **2017** *113*, 250–256 http://dx.doi.org/10.1016/j.geomphys.2016.07.006
12. Samokhin A.V. On periodic boundary solutions for cylindrical and spherical KdV-Burgers equations. *arXiv:2011.14189 [nlin.PS]*, **2020**, 10 p.

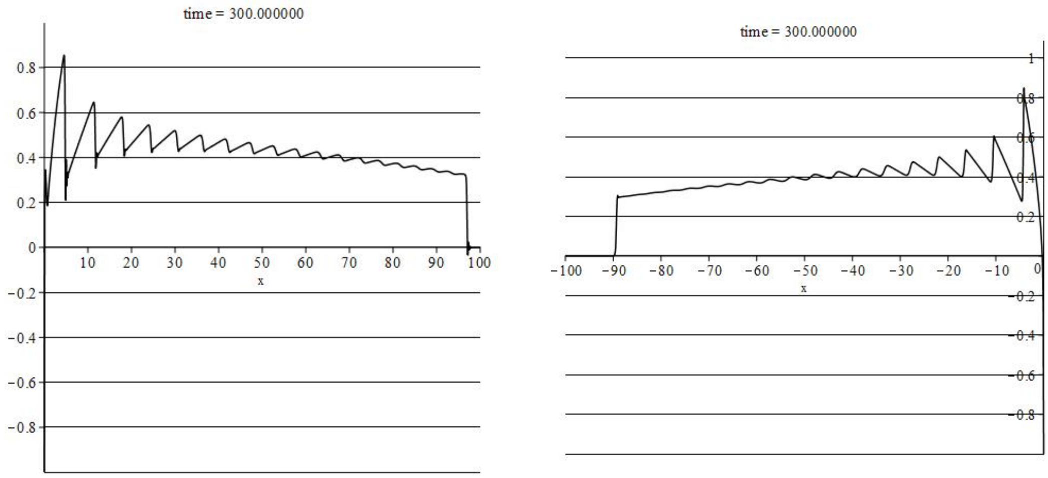

Figure 4. *Spherical KdV-Burgers,* $u_0 = \sin t$*,* ***Left****:* $t = 300, \varepsilon = 0.1, \delta = 0.001$. ***Right****:* $u \leftrightarrow -u, t = 300, \varepsilon^2 = 0.02, \delta = 0.001\ \varepsilon^2 = 0.2$

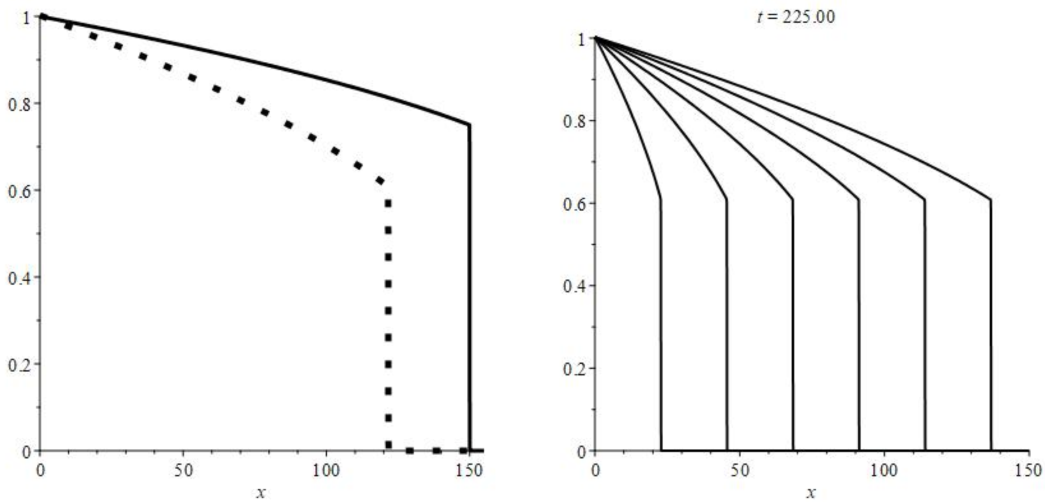

Figure 5. *Constant boundary solutions to Burgers equation,* $\varepsilon = 0.1, t = 200$*.* ***Left****: Solid line — cylindrical, dots line — spherical.* ***Right****: A trace of movement to the right of the spherical solution at moments* $t = 37.5 \cdot k, k = 1 \ldots 6$

Preprints (www.preprints.org) | NOT PEER-REVIEWED | Posted: 23 December 2020 doi:10.20944/preprints202012.0579.v1

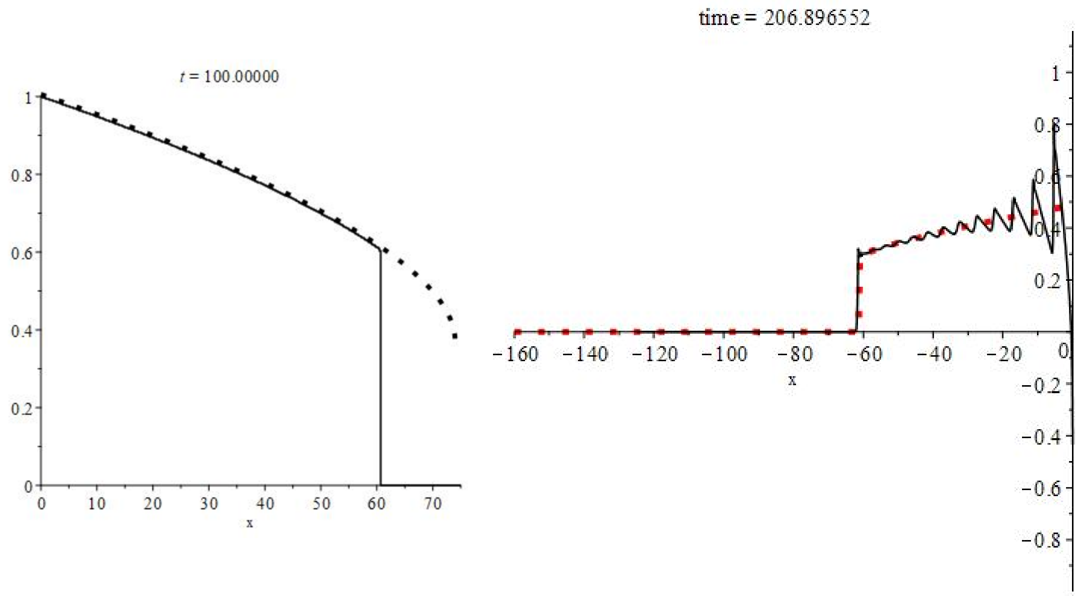

Figure 6. ***Left***: *Solid line — solution to* (17)*, dots line — its* u_2 *approximation.* ***Right***: *Solid line— solution to spherical KdV,* $x \to -x$*,* $\varepsilon^2 = 0.02$*,* $\delta = 0.002$*, dots line — its* $\tilde{u}_2$ *approximation; both at* $t = 200$.

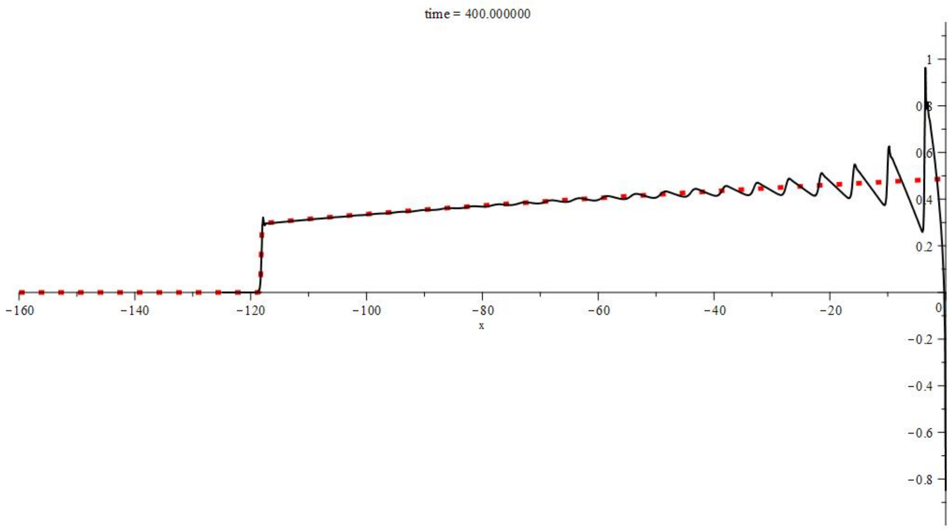

Figure 7. Solid line— solution to spherical KdV, $x \to -x$, $\varepsilon^2 = 0.02$, $\delta = 0.002$, dots line — its $\tilde{u}_2$ approximation; both at $t = 400$.